Spatial switching in chemical reactions with heterogeneous catalysis

R. M. Shymko and Leon Glass

Institute for Fundamental Studies, Department of Physics and Astronomy, The University of Rochester, Rochester, New York 14627
(Received 27 August 1973)

The qualitative properties of chemical systems with localized (heterogeneous) catalysts can depend on the relative locations of the catalysts. By considering some simple chemical systems with two catalytic sites it is shown that the number and the stability of steady states and cycles changes with intercatalytic separation. These examples indicate that geometrical considerations must be explicitly considered when analyzing the dynamics of highly structured (e.g., biological) systems.

I. INTRODUCTION

Few naturally occurring chemical reactions occur in well-stirred homogeneous phases. When more realistic reaction conditions are considered, whole new classes of possibilities for the dynamics of reacting chemical systems emerge. If a system is not well stirred, and the effects of diffusion are explicitly considered, it is known that for open systems, the homogeneous phase can become unstable, leading to the development of spatial and temporal periodicities.[1-4] Since these structures are maintained at the expense of energy flow through the system, they have been called *dissipative structures*.

In addition, many chemical systems are spatially heterogeneous, with reactions rates varying in space as a consequence of such structural features of the chemical system as surfaces, impurities, gradients of concentration, and heterogeneous catalysts. These factors can have major effects on the dynamics of chemical systems. For example, it has recently been shown that gradients of concentration can lead to the observation of propagating chemical waves, for cases in which waves are not otherwise found.[5] In addition, in homogeneously oscillating chemical systems, heterogeneous catalysts can induce waves and thus act as pacemakers.[6] In another study of the effects of heterogeneous catalysis in open systems, it was shown that time independent undulatory inhomogeneities can occur in the region of the catalysts even though no instabilities were found for the homogeneous system in the absence of catalysts.[7] In a computer study of chemical systems with catalysts localized in compartments between which diffusion can freely occur, it was shown that the qualitative dynamics (the number of steady states and their stability) can depend on the relative positions of the localized sites.[8] For example, the appearance of stable limit cycle oscillations was found for certain ranges of catalyst separation for open systems with two localized sites, and the appearance of completely new dynamical modes was observed as a function of the spatial arrangements of catalysts in open systems with three catalytic sites. In an analytic study of the effects of intercatalytic separation on the stability of steady states, it was confirmed that changes in catalyst separation can alter the stability of the steady state.[9]

By *spatial switching* we refer to those changes in the qualitative dynamics of a system which are induced by an alteration of the geometry of the system. A value of the parameters at which the change in qualitative dynamics occurs is called a *bifurcation point*.[10] In the following we demonstrate spatial switching in chemical systems with two localized, but chemically coupled catalytic sites. In Sec. II, we adopt the equations for heterogeneous catalysis proposed by Ortoleva and Ross[6,7] assuming that the catalysts display the nonlinear dependence on the concentration of chemical species typical of biochemical systems.[8] The variation of the number of steady states on catalyst separation is studied in Sec. III. In Sec. IV we analyze the dependence of the stability of these steady states as a function of catalyst separation. The results are discussed in Sec. V.

II. EQUATIONS FOR HETEROGENEOUS CATALYSIS

The equations for systems displaying heterogeneous catalysis are[6,7]

$$\partial\Psi/\partial t + F(\Psi) - D\nabla^2\Psi = G(\Psi)\Delta(\mathbf{r}) \,, \tag{1}$$

where $\Psi(\mathbf{r}, t)$ is a column vector of concentrations, D is a matrix of diffusion coefficients, F gives the change in concentrations due to homogeneous chemical reactions, G gives the localized changes in concentrations due to catalytic activity, and $\Delta(\mathbf{r})$ is a diagonal matrix of Dirac δ functions, $\Delta_{ij} = \delta_{ij}\delta(\mathbf{r} - \mathbf{r}_i)$, giving the location of catalytic sites. In general, the terms F and G are nonlinear and integration of this equation for given boundary conditions is impossible. In order to display the phenomenon of spatial switching, we have assumed a special case of Eq. (1) which is suitable for (though not necessarily limited to) the analysis of biochemical networks. The range of effects we observe should also be found in more complicated systems. We assume there are two chemical species in a one dimensional system with boundary conditions $\Psi(\mathbf{r}, t)|_{|\mathbf{r}|\to\infty} = 0$ and a diagonal diffusion matrix, $D_{ij} = D_i\delta_{ij}$. Each chemical undergoes a spatially homogeneous decay at a rate γ_i proportional to its concentration. The system is assumed to be open and far from equilibrium. Synthesis of the chemical species occurs *only* at the localized catalysts, at a rate determined by the concentration of control chemicals.[11] This dependence, which has been observed in a number of different biochemical systems, can be empirically described by the Hill function[12,13]

$$f_A(\Psi) = \frac{b + (\Psi/\theta)^n}{1 + (\Psi/\theta)^n} \ , \quad b < 1 \ , \tag{2a}$$

where n, b, and θ are positive, real constants which are fit to experimental data. Equation (2a) is a bounded monotonic increasing function which corresponds to the *activation* of production by the control chemical Ψ. If Ψ *inhibits* the production of its target compound, the corresponding form is

$$f_I(\Psi) = \frac{1 + b(\Psi/\theta)^n}{1 + (\Psi/\theta)^n} \ , \quad b < 1 \ , \tag{2b}$$

which is a bounded, monotonic decreasing function of Ψ. We assume the two chemical species are chemically coupled, mutually controlling the production rate of the other compound via functions displayed in Eqs. (2). The resulting equations describing heterogeneous catalysis for this system (in one dimension) are then

$$\partial\Psi_1/\partial t + \gamma_1\Psi_1 - D_1\,\partial^2\Psi_1/\partial x^2 = \lambda_1 f_1[\Psi_2(x,\ t)]\,\delta(x - x_1), \tag{3a}$$

$$\partial\Psi_2/\partial t + \gamma_2\Psi_2 - D_2\,\partial^2\Psi_2/\partial x^2 = \lambda_2 f_2[\Psi_1(x,\ t)]\,\delta(x - x_2) \ , \tag{3b}$$

where λ_i is the maximal synthetic rate of species i, and x_i is the site where species i is synthesized. Equations (3) will be analyzed for the three types of coupling between the two chemical species: mutual activation, mutual inhibition, and activation–inhibition.

III. THE NUMBER OF STEADY STATES

If we set the time derivatives in Eqs. (3) equal to zero, each of the resulting equations for the steady-state solutions becomes the equation for the Green's function of a modified Helmholtz equation, the solution of which is well-known.[14] Thus, we obtain the equations for the steady-state solutions, $\Psi_1^0(x)$ and $\Psi_2^0(x)$:

$$\Psi_1^0(x) = \frac{\lambda_1\kappa_1}{2\gamma_1}\, e^{-\kappa_1|x-x_1|} f_1(\Psi_2^0(x_1)) \ , \tag{4a}$$

$$\Psi_2^0(x) = \frac{\lambda_2\kappa_2}{2\gamma_2}\, e^{-\kappa_2|x-x_2|} f_2(\Psi_1^0(x_2)) \ , \tag{4b}$$

where

$$\kappa_i = (\gamma_i/D_i)^{1/2}, \quad i = 1,\ 2 \ . \tag{4c}$$

Note that the steady-state concentrations are peaked at their production points and are damped exponentially away from these points.

Equations (4) show that the complete space-dependent solutions are determined by the values of Ψ_1^0 and Ψ_2^0 at the points x_2 and x_1, respectively. Hence, we can set $x = x_2$ in Eq. (4a) and $x = x_1$ in Eq. (4b) to obtain:

$$y_1 = \beta_1 f_1(y_2), \tag{5a}$$

$$y_2 = \beta_2 f_2(y_1) \ , \tag{5b}$$

where $y_1 = \Psi_1^0(x_2)$, $y_2 = \Psi_2^0(x_1)$, and $\beta_i = (\lambda_i\kappa_i/2\gamma_i)\exp(-\kappa_i d)$, with $d = |x_1 - x_2|$. The steady states of the system are found by solving Eqs. (5) for y_1 and y_2. If the complete space dependent solutions are desired, we can substitute the solutions of Eqs. (5) back into Eqs. (4).

To analyze spatial switching, the parameter of primary interest is d, the separation between the two production points. Therefore, to clarify the dependence of the dynamics on d and to simplify the analysis, we will consider a system with the properties

$$\begin{aligned} &\gamma_1 = \gamma_2 = \gamma, \\ &D_1 = D_2 = D, \\ &\lambda_1 = \lambda_2 = \lambda, \\ &\beta_1 = \beta_2 = \beta. \end{aligned} \tag{6}$$

This simplified system exhibits the same qualitative behavior as the original system.

Three possibilities exist for the coupling between the two system components: mutual activation, mutual inhibition, and activation–inhibition. For mutual activation and mutual inhibition, we make the further simplification that $f_1 = f_2 = f$.

A. Mutual activation

With the above assumptions, Eqs. (5) become

$$y_1 = \beta f(y_2) \ , \tag{7a}$$

$$y_2 = \beta f(y_1). \tag{7b}$$

The curves (7a) and (7b), plotted in the $y_1 - y_2$ phase plane, are the reflections of each other through the symmetry axis $y_1 = y_2$. Consequently, a solution to Eqs. (7) occurs wherever one of the sigmoidal curves crosses the symmetry axis. There may be one or three intersections of the two curves, depending on the parameters. A graphical solution of Eqs. (7), showing three steady states, is given in Fig. 1.[15] From Fig. 1 we see that three steady states will exist if and only if, at some steady state the slope, dy_1/dy_2, of Eq. (7a) is greater than the slope, dy_1/dy_2, of Eq. (7b). This condition for the existence of three steady states can be written as

$$\beta \left.\frac{df(y)}{dy}\right|_{y=y_s} > 1 \ , \tag{8}$$

where y_s is a solution of Eqs. (7). Note that condition

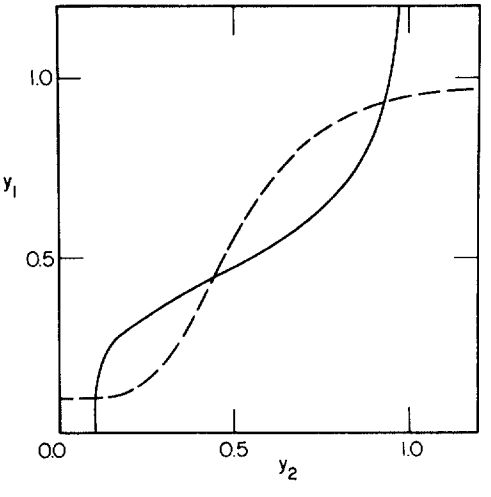

FIG. 1. Graphical solution for the steady states of Eq. (7) for the case of mutual activation in which the functions $f(y)$ are given in Eq. (2a) with $\theta = 0.5$, $b = 0.1$, $n = 4$ [these parameters are also used in constructing Figs. (2)–(7)], and $\beta = 1$. The dashed line (- - - -) gives Eq. (7a) and the solid line (——) gives Eq. (7b).

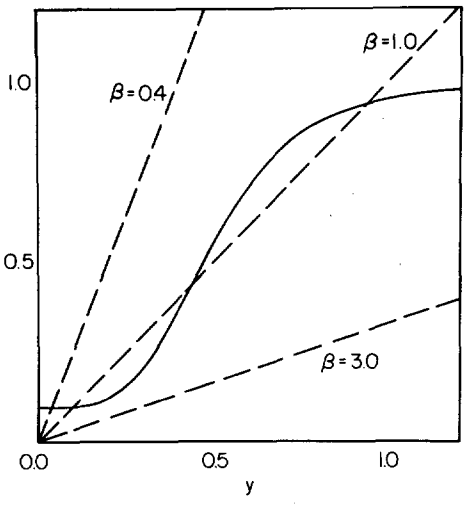

FIG. 2. Graphical solution of Eq. (9) for three values of β with $f(y)$ given in Eq. (2a). The solid line gives $f(y)$, and the dashed line y/β.

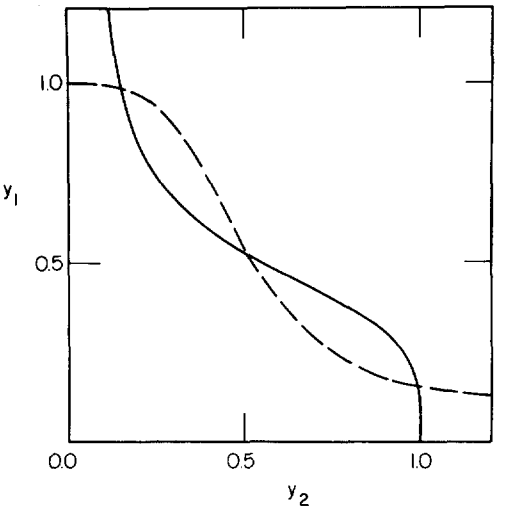

FIG. 4. Graphical solution for the steady states of Eq. (7) for the case of mutual inhibition, in which the functions $f(y)$ are given in Eq. (2b) and $\beta=1$. The dashed line gives Eq. (7a) and the solid line Eq. (7b).

(8) will hold only at the central steady state and *not* at the outer steady states.

The steady states of the system always occur on the line $y_1=y_2$. Consequently, the solutions of Eqs. (7) on the line $y_1=y_2$ are the same as the solutions of the equation

$$y/\beta=f(y)\ . \tag{9}$$

Figure 2 shows the graphical solution of Eq. (9) for different values of β. We see that there are three distinct ranges of β: a high and a low range in which only one steady state exists, and an intermediate range in which three steady states exist.

The plot of the solutions, y_s, of Eq. (9) versus β is given in Fig. 3. In the region where three steady states exist, the steady state values of y_1 and y_2 *both* lie on the upper, middle, or lower branch of the curve. The middle branch (dashed line) will be shown later to represent an unstable steady state. Notice that the shape of the curve in Fig. 3 depends only on the normalized response function, f. For functions f which are not steep enough to satisfy Eq. (8), the plot of y_s versus β will be single-valued for all β.

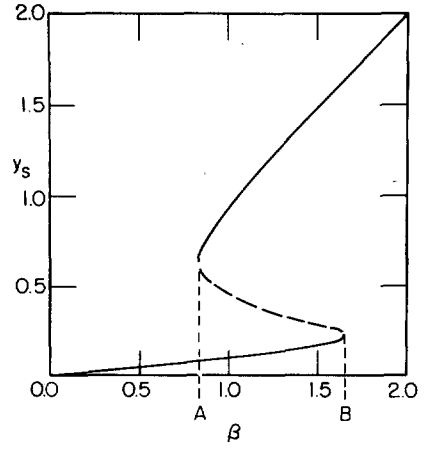

FIG. 3. The steady states of Eq. (7) for the case of mutual activation as a function of β. The dashed line represents unstable steady states and the solid line represents stable steady states. At a steady state both y_1 and y_2 take the same value, y_s.

In Fig. 3, there are two bifurcation points, A and B. Since β depends exponentially on the separation of the production points, separations $d=\infty$ and $d=0$ correspond to the points $\beta=0$ and $\beta=\beta_0=\lambda\kappa/2\gamma$, respectively. Therefore, as d is increased from zero to infinity, the system may pass through zero, one, or two bifurcation points, depending on the value of β_0.

For the function f exhibited in Fig. 2

$$\lim_{y\to 0} f(y)/y > 0\ . \tag{10}$$

For other functions such that this limit goes to zero [for example, if $b=0$ in equation (2a)], the point B in Fig. 3 moves toward $\beta=\infty$ and only one bifurcation point A remains.

B. Mutual inhibition

Since f is monotonically decreasing, it has exactly one intersection with the symmetric axis $y_1=y_2$ and there is one solution of Eq. (7) where $y_1=y_2$. However, in this case there may be two more solutions off the symmetric axis. A graphical solution of Eqs. (7), showing three steady states, is given in Fig. 4. Here, there will be three steady states if and only if the slope, dy_1/dy_2, of Eq. (7a) is less than the slope, dy_1/dy_2, of Eq. (7b) at the steady state, $y_1=y_2$. This will occur if

$$\beta\left.\frac{df(y)}{dy}\right|_{y=y_S} < -1\ . \tag{11}$$

In Fig. 5 we show the graphical solution of Eq. (9) for the steady state in which $y_1=y_2$. If the line y/β intersects $f(y)$ in the region between the cross bars, Eq. (11) holds and three steady states will exist.

Figure 6 shows the steady states as a function of β.

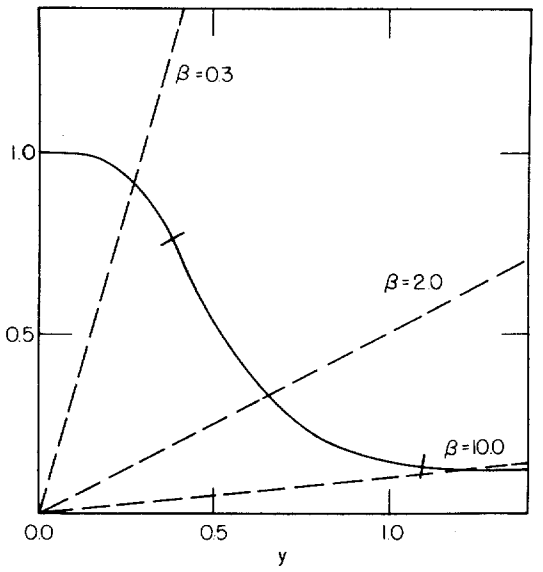

FIG. 5. Graphical solution of Eq. (9) for three values of β with $f(y)$ given in Eq. (2b). The solid line gives $f(y)$ and the dashed line gives y/β. If the two curves intersect between the cross bars there will be three steady states.

If the system is at one of the stable steady states in the region of three steady states, one of the concentrations y_1 or y_2 takes the value on the upper branch of the curve and the other takes the value on the lower branch. At the second stable steady state, the values of y_1 and y_2 are reversed. At all other steady states, including the unstable steady state in the intermediate region (dashed line), both concentrations have equal values as given in the graph.

In Fig. 6 we see two bifurcation points, A and B. Just

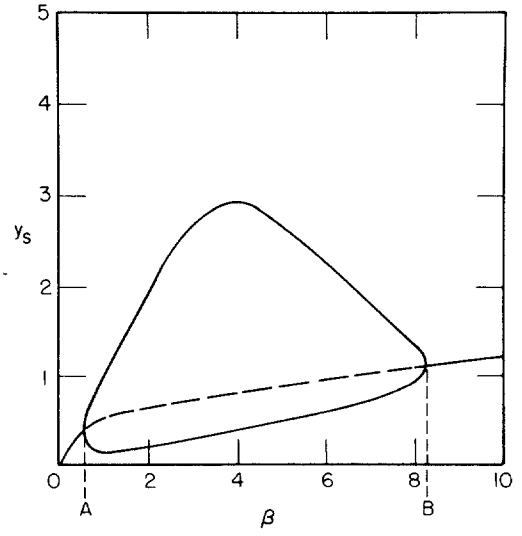

FIG. 6. The steady states of Eq. (7) for the case of mutual inhibiton as a function of β. The dashed line represents unstable steady states and the solid line stable steady states. At a stable steady state in the three steady state region, one of the concentrations lies on the upper stable branch, and the other lies on the lower stable branch.

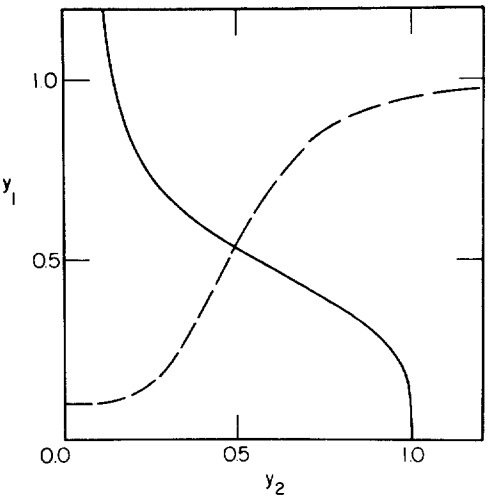

FIG. 7. Graphical solution for the steady states of Eq. (5) for the case of activation–inhibition, in which f_1 is given in Eq. (2a) and f_2 is given in Eq. (2b). The dashed line gives Eq. (5a) and the solid line Eq. (5b).

as in the case of mutual activation, the system may pass through zero, one, or two of these points, depending on the value of β_0, as d is increased from zero to infinity. Both bifurcation points disappear if Eq. (11) is never satisfied, and the plot of y_s versus β will be single-valued for all β.

For the function f shown in Fig. 5,

$$\lim_{y\to\infty} yf(y) = \infty \ . \tag{12}$$

If this limit, instead, goes to zero [for example, by letting b go to zero in Eq. (2b)], the bifurcation point B in Fig. 6 moves toward $\beta = \infty$ and only A remains.

C. Activation-inhibition

A graphical solution of Eqs. (5) for this case is given in Fig. 7. There is exactly one intersection of the curves in the phase plane, with no possibility of multiple steady states. The single steady states can be stable or unstable, depending on the values of the parameters.

IV. STABILITY OF THE STEADY STATE

We are interested in determining the stability of each of the steady states found in the previous section. To do the analysis, we employ standard techniques[16] and compute the asymptotic time dependence of small deviations $\epsilon(x, t)$ away from the steady state,

$$\Psi_i(x, t) = \Psi_i^0(x) + \epsilon_i(x, t), \quad (i = 1, 2), \tag{13}$$

by considering the equations of motion linearized about the steady state. In general, the asymptotic time dependence of any function, $h(t)$, can be found from its Laplace transform

$$\tilde{h}(s) = \int_0^\infty e^{-st} h(t)\, dt \ . \tag{14}$$

Since the inverse Laplace transform is

$$h(t) = \frac{1}{2\pi i} \int_{c-i\infty}^{c+i\infty} e^{st} \tilde{h}(s) ds \ , \tag{15}$$

where c is a real number greater than the real part of

any singularity of $\bar{h}(s)$ in the complex s plane, the dominant behavior of $h(t)$ as $t \to \infty$ will be given by $h(t) \sim e^{s_0 t}$ where s_0 is the value of the pole in the complex s plane having the largest real part. If there are any poles of $h(s)$ in the right half of the complex s plane (Re $s_0 > 0$), then $h(t)$ diverges. If the linearizations about the steady states diverge in time, then the steady state is said to be unstable. In the following, we show that for the two cases of mutual activation and mutual inhibition there will be unstable steady states only in the region of multiple steady states, with the central branch in Figs. 3 and 6 being unstable. For activation–inhibition the stability of the steady state depends on the parameters.

By employing the Green's function for Eq. (3)[17,18]

$$G_i(x, x'; t, t') = \frac{\exp[-\gamma_i(t-t') - (x-x')^2/4D_i(t-t')]}{[4\pi D_i(t-t')]^{1/2}}, \quad (i = 1, 2), \tag{16}$$

the solutions can be explicitly written

$$\Psi_1(x, t) = \lambda_1 \int_0^t dt' G_1(x, x_1; t, t') f_1[\Psi_2(x_1, t')] + \int_{-\infty}^{\infty} dx' G_1(x, x'; t, 0)\Psi_1(x', 0), \tag{17a}$$

$$\Psi_2(x, t) = \lambda_2 \int_0^t dt' G_2(x, x_2; t, t') f_2[\Psi_1(x_2, t')] + \int_{-\infty}^{\infty} dx' G_2(x, x'; t, 0)\Psi_2(x', 0). \tag{17b}$$

The nonlinear production terms in the first terms of the right hand sides of Eqs. (19) are linearized about the steady states as follows:

$$f_j[\Psi_i(x_j, t)] = f_j[\Psi_i^0(x_j)] + \alpha_j \epsilon_i(x_j, t) + \cdots, \tag{18}$$

where

$$\alpha_j = \left.\frac{df_j[\Psi_i(x_j)]}{d\Psi_i(x_j)}\right|_{\Psi_i(x_j)=\Psi_i^0(x_j)}. \tag{19}$$

Substituting into Eqs. (17), where the concentration of chemicals 1, 2, are considered explicitly only at the points x_2, x_1, respectively, and noticing that $G(x, x'; t, t') = G(|x-x'|; t-t')$ we find

$$\epsilon_1(x_2, t) = \lambda_1\alpha_1 \int_0^t dt' G_1(d; t-t')\epsilon_2(x_1, t') + \int_{-\infty}^{\infty} dx' G_1(x_2 - x'; t)\epsilon_1(x', 0), \tag{20a}$$

$$\epsilon_2(x_1, t) = \lambda_2\alpha_2 \int_0^t dt' G_2(d; t-t')\epsilon_1(x_2, t') + \int_{-\infty}^{\infty} dx' G_2(x_1 - x')\epsilon_2(x', 0), \tag{20b}$$

where d is the intercatalytic distance $|x_1 - x_2|$.

Using the convolution theorem for Laplace transforms, we compute the Laplace transforms of Eqs. (20)

$$\tilde{\epsilon}_1(x_2, s) = \lambda_1\alpha_1\tilde{G}_1(d; s)\tilde{\epsilon}_2(x_1, s) + \tilde{g}_1(x_2, s), \tag{21a}$$

$$\tilde{\epsilon}_2(x_1, s) = \lambda_2\alpha_2\tilde{G}_2(d; s)\tilde{\epsilon}_1(x_2, s) + \tilde{g}_2(x_1, s), \tag{21b}$$

where $g_1(x_2, s)$ and $g_2(x_1, s)$ are the transforms of the last terms of the right-hand sides of Eqs. (20). These linear algebraic equations in $\tilde{\epsilon}_1(x_2, s)$ and $\tilde{\epsilon}_2(x_1, s)$ are easily solved to obtain

$$\tilde{\epsilon}_1(x_2, s) = \frac{\tilde{g}_1(x_2, s) + \lambda_1\alpha_1\tilde{G}_1(d; s)\tilde{g}_2(x_1, s)}{1 - \lambda_1\lambda_2\alpha_1\alpha_2\tilde{G}_1(d; s)\tilde{G}_2(d; s)}, \tag{22a}$$

$$\tilde{\epsilon}_2(x_1, s) = \frac{\tilde{g}_2(x_1, s) + \lambda_2\alpha_2\tilde{G}_2(d; s)\tilde{g}(x_2, s)}{1 - \lambda_1\lambda_2\alpha_1\alpha_2\tilde{G}_1(d; s)\tilde{G}_2(d; s)}. \tag{22b}$$

Notice that $g_1(x_2, t)$ and $g_2(x_1, t)$ represent the time evolution of the system in the absence of catalysts, starting from initial values $\epsilon_1(x, 0)$ and $\epsilon_2(x, 0)$. Without catalysts, there is no net production of the system components and therefore, since decay is present, $g_1(x_2, t)$ and $g_2(x_1, t)$ must be decreasing functions of t for any transport mechanism. This means that $\tilde{g}_1(x_2, s)$ and $\tilde{g}_2(x_1, s)$ have no singularities in the right half s plane and hence, stability is determined by the position of the zeros of the denominators, i.e., by the complex solutions of

$$1 - \lambda_1\lambda_2\alpha_1\alpha_2\tilde{G}_1(d; s)\tilde{G}_2(d; s) = 0. \tag{23}$$

The Laplace transform of the Green's function given in Eq. (16) (with $x - x' = d$) is

$$\tilde{G}(d; s) = (2D)^{-1}\left(\frac{s+\gamma}{D}\right)^{-1/2} \exp\left[-\left(\frac{s+\gamma}{D}\right)^{1/2} d\right]. \tag{24}$$

Inserting this into Eq. (23), we obtain, after some manipulation.

$$z - \xi e^{-2d\rho^{1/2} z^{1/2}} = 0, \tag{25}$$

where

$$z = (s+\gamma)/\rho D,$$

$$\rho = (\lambda^2/4D^2)|\alpha_1\alpha_2|,$$

$$\xi = +1 \quad \alpha_1\alpha_2 > 0 \text{ (mutual activation or inhibition)}$$

$$= -1 \quad \alpha_1\alpha_2 < 0 \text{ (activation–inhibition)}.$$

The asymptotic time behavior of $\epsilon_1(x_2, t)$ and $\epsilon_2(x_1, t)$ is given by

$$\epsilon_1, \epsilon_2 \sim e^{-\gamma(1-\rho z_0/\kappa^2)t}, \tag{26}$$

where z_0 is the solution of Eq. (25) which is farthest right in the complex z plane and $\kappa = (\gamma/D)^{1/2}$. Therefore, the condition for instability is

$$\rho \mathrm{Re} z_0/\kappa^2 > 1. \tag{27}$$

As $2d\rho^{1/2}$ increases, the roots of Eq. (25) follow the trajectories given in Fig. 8, (see Appendix). Two new (complex conjugate) zeros appear at $z = -1$ whenever $2d\rho^{1/2}$ reaches the value $(4n - \xi - 1)(\pi/2)$ for successive positive integers n. Every trajectory eventually crosses over into the right half-plane, but the maximum positive real part attained by each one is smaller than that of the previous one by a factor greater than $e^{2\pi}$. Therefore, we need only consider the lowest order ($n = 0$) trajectory.

For the case of mutual activation and mutual inhibition, ($\xi = +1$), the $n = 0$ root lies on the positive real axis. Using the identity

$$(\rho/\kappa^2)e^{-2\kappa d} \equiv \beta^2|\alpha_1\alpha_2|, \tag{28}$$

Eq. (25) can be rewritten

$$(\rho z/\kappa^2)\exp\{2\kappa d[(\rho z/\kappa^2)^{1/2} - 1]\} = \beta^2|\alpha_1\alpha_2|. \tag{29}$$

The left hand side is monotonic in z and is equal to 1 when $\rho z/\kappa^2$ is equal to 1. Therefore, if

$$\beta^2|\alpha_1\alpha_2| > 1, \tag{30}$$

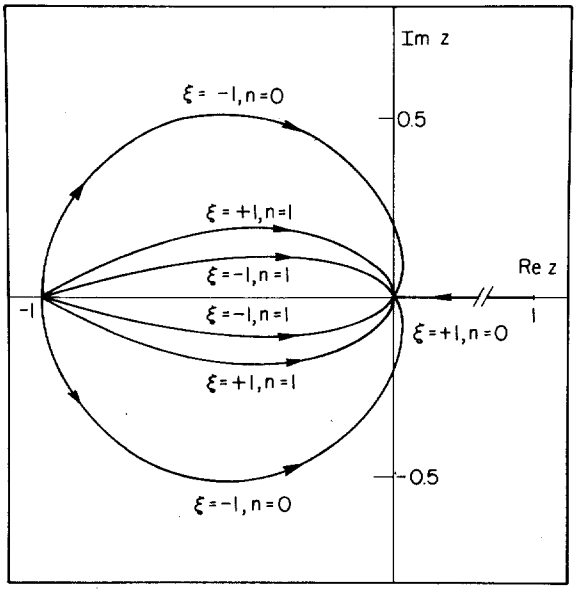

FIG. 8. Trajectories of solutions of Eq. (25) in the complex z plane found using Eq. (A6). Curves labelled $\xi = +1$ refer to mutual activation or inhibiton and those labelled $\xi = -1$ refer to activation–inhibition. The $n = 0$, $n = 1$ trajectories are plotted for both cases.

we must have $\rho z_0/\kappa^2 > 1$, where z_0 is the (real) solution of Eq. (30), and from Eq. (27), the steady state is unstable.[17] Equation (30) is equivalent to the conditions for the existence of three steady states, Eqs. (8) and (11). Further, since Eqs. (8) and (11) are only satisfied for the central branch in Figs. (3) and (6), we observe that the central branch gives unstable steady states and all other steady states are stable.

For the case of activation–inhibition ($\xi = -1$), the $n = 0$ trajectory of Eq. (25) lies off the real axis in the complex z plane. The analysis of Eq. (25) for this case is not simple (see Appendix) and an analytic stability criterion analogous to Eq. (30) has not been found. However, Re $z_0 > 0$ only if

$$2d\rho^{1/2} > (\pi/\sqrt{2})\, e^{\pi/4}. \tag{31}$$

Therefore, Eq. (31) is a necessary, but not sufficient, condition for Eq. (27) to hold. In general for catalytic systems with activation–inhibition, the function $2d\rho^{1/2}$ increases from 0, passes through a maximum, and decreases again as the intercatalytic separation increases from $d = 0$. Consequently, for systems in which unstable regions are found, a typical behavior is that there will be a range of separations for which the steady state is unstable, with stability found at both larger and smaller separations. We have chosen a set of parameters of Eq. (17) for which the steady state is unstable. By integrating Eq. (17) numerically, starting from a variety of initial conditions, we have found the system assumes a limit cycle oscillation, independent of the initial conditions. An example, is given in Fig. 9.

V. DISCUSSION

We have shown that the qualitative dynamics of chemical systems with heterogeneous catalysis depends in a fundamental way on the relative locations of the catalytic sites. Some simple examples were given in which changes in the relative locations of catalytic sites lead to the appearance of multiple steady states and stable limit cycle oscillations.

These results are important for the study of biological systems. Here it is known that catalysts are localized on membranes and that structural integrity at the cellular and subcellular level is often necessary for proper functioning. Further, stable cycles have been observed in diverse biological systems,[19,20] and the existence of multiple steady states in gene networks may be important in the understanding of the biochemical basis for differentiation.[21,22] Consequently, in theoretical analyses of biological systems, explicit consideration must be made of geometrical factors which may influence the dynamical behavior of the system. For example, changes in the morphological states of mitochondria might lead to changes in observed metabolic pathways in the mitochondria in different spatial configurations.[9]

As the number of catalytic sites increases, theoretical analysis becomes progressively more difficult, but the range of interesting behavior also increases. In a recent computer study of the dynamics of compartmentalized catalytic networks with more than two chemically coupled sites, correspondence was found between the dynamics of chemical systems and the behavior of analogous Boolean switching networks in which the continuous Hill functions, Eq. (2), are replaced by discrete on-off switches, and the time lags due to diffusion in the

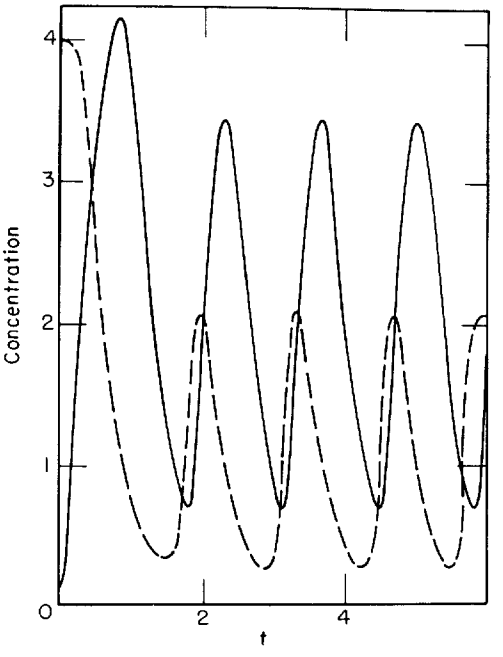

FIG. 9. Limit cycle solution of Eqs. (3) found for the case of activation–inhibition, where f_1 is given in Eq. (2a) and f_2 is given in Eq. (2b). The dashed curve gives $\Psi_1(x_2, t)$ and the solid curve gives $\Psi_2(x_1, t)$. The solution was found by integrating Eq. (17) numerically, with initial conditions $\Psi_1(x, 0) = 4.0$, $\Psi_2(x, 0) = 0.1$ (for all x), and all other parameters equal for both components and given by $\gamma = 2$, $D = 2$, $\lambda = 54$, $\theta = 1.0$, $b = 0.0$, $n = 8$, with the intercatalytic distance $|x_1 - x_2| = 1$. With these parameters Re s_0 is approximately 3.6.

chemical systems lead to time lags along relay lines in the equivalent Boolean systems.[23] This close correspondence suggests the possibility that simple chemical computers and chemical automata can be synthesized in the laboratory by constructing chemical systems with several localized catalytic sites.

To our knowledge, there have been no demonstrations of spatial switching in laboratory systems. The synthesis of such systems would be of intrinsic interest, would help provide an experimental basis for the understanding of the coupling between structure and dynamics in biological systems, and may be a necessary first step in the design of chemical computers. We hope the analysis presented here will provide an impetus for the laboratory synthesis of chemical systems displaying spatial switching.

ACKNOWLEDGMENT

This research has been partially supported by NSF grant GU-4040.

APPENDIX

The stability of the steady state of Eq. (17) is determined by finding the solution of Eq. (25) which has the largest real part and applying Eq. (27). Equation (25) is rewritten as

$$z - \xi e^{-\eta z^{1/2}} = 0 , \tag{A1}$$

where $\xi = \pm 1$ and $\eta = 2d\rho^{1/2}$. Taking the logarithm of Eq. (A1) we find

$$\log z = -\eta z^{1/2} \pm i(\pi/2)(4n+1-\xi), \quad n = 0, 1, 2, \cdots, \tag{A2}$$

where the + or − sign locates the root in the upper or lower half-plane, respectively. Substituting $z = re^{i\theta}$ and equating the real and imaginary terms in Eq. (A2), we find

$$\log r = -\eta r^{1/2} \cos\tfrac{1}{2}\theta , \tag{A3}$$

$$\theta = -\eta r^{1/2} \sin\tfrac{1}{2}\theta \pm \tfrac{1}{2}\pi(4n+1-\xi) . \tag{A4}$$

We will choose the range of θ to be $-\pi \le \theta \le \pi$ so that, if $\xi = 1$ (mutual activation or inhibition) and $n = 0$, Eq. (A4) requires $\theta = 0$. Consequently, this root is real, $z = r$, with

$$r = e^{-\eta r^{1/2}}, \quad \theta = 0 . \tag{A5}$$

If $n + 1 - \xi \neq 0$, the equation for the trajectories of the roots, obtained by eliminating η between Eqs. (A3) and (A4), is

$$r = e^{-[\pm\pi(4n+1-\xi)/2 - \theta]\cot\theta/2}, \quad n + 1 - \xi \neq 0 . \tag{A6}$$

These trajectories are plotted in Fig. 8.

Each point on a trajectory defines a value of η, which can be obtained by substituting the values of r and θ satisfying Eq. (A6) back into Eqs. (A3) and (A4). By substituting $\theta = \pi$ into Eqs. (A3) and (A4), we see that, except for $n = 0$, $\xi = +1$, the nth-order trajectories appear at $z = -1$ when η passes through the value

$$\eta = \tfrac{1}{2}\pi(4n - 1 - \xi) . \tag{A7}$$

Similarly, substituting $\theta = \pi/2$ into these equations, we find that the trajectories pass into the right half-plane when

$$\eta = (4n - \xi)(\pi/\sqrt{2})\, e^{(4n-\xi)\pi/4} . \tag{A8}$$

[1] A. M. Turing, Philos. Trans. R. Soc. Lond. B **237**, 37 (1952).
[2] J. I. Gmitro and L. E. Seriven, in *Intracellular Transport*, edited by K. B. Warren (Academic, New York, 1966).
[3] I. Prigogine and G. Nicolis, J. Chem. Phys. **46**, 3542 (1967).
[4] I. Prigogine and P. Lefever, J. Chem. Phys. **48**, 1695 (1968).
[5] N. Kopell and L. H. Howard, Science **180**, 1171 (1973).
[6] P. Ortoleva and J. Ross, J. Chem. Phys. **58**, 5673 (1973).
[7] P. Ortoleva and J. Ross, J. Chem. Phys. **56**, 4397 (1972).
[8] L. Glass and S. A. Kauffman, J. Theor. Biol. **34**, 219 (1972).
[9] H. D. Thames, J. Theor. Biol. **41**, 331 (1973).
[10] A. A. Andronov, E. A. Leontovich, I. I. Gordon, and A. G. Maier, *Theory of Bifurcations of Dynamical Systems on a Plane* (U. S. Department of Commerce, National Technical Information Service, Springfield, VA, 1971).
[11] A more detailed discussion of these assumptions and their applicability to the analysis of biochemical networks can be found in Ref. 8.
[12] J. Monod, J. Wyman, and J. Changeux, J. Mol. Biol. **12**, 88 (1965).
[13] G. Yagil and E. Yagil, Biophys. J. **11**, 11 (1971).
[14] G. Arfken, *Mathematical Methods for Physicists* (Academic, New York, 1966), p. 606.
[15] Figures 1–7 are computed for the Hill functions, Eqs. (2), with $b = 0.1$, $\theta = 0.5$, $n = 4$. The qualitative features of the figures, the number of steady states and their stability remain invariant under substitutions of other monotonic, sigmoidal functions.
[16] See, for example, A. M. Krall, *Stability Techniques for Continuous Linear Systems* (Gordon and Breach, New York, 1967), Chap. III.
[17] P. M. Morse and H. Feshbach, *Methods of Theoretical Physics* (McGraw-Hill, New York, 1953), p. 1593.
[18] P. Ortoleva and J. Ross, Proceedings of the Conference on Dissipative Structures, Membranes and Evolution, Bruxelles, 1972; H. D. Thames, Bull. Math. Biophys. (to be published). These papers discuss the use of Green's functions to derive ordinary nonlinear integral equations which are equivalent to the nonlinear partial differential equations given in Eq. (1), and suggest that the analysis of the steady states and stability of Eq. (1) can be accomplished using the integral representation. It should be noted that the steady state equations, Eqs. (4), can be derived from Eq. (17) by considering the limit $t \to \infty$.
[19] B. Chance, R. Estabrook, and A. Ghosh, Proc. Natl. Acad. Sci. USA **51**, 1244 (1966).
[20] R. R. Klevecz, Science **166**, 1536 (1969).
[21] J. Monod and F. Jacob, Cold Spring Harbor Symp. Quant. Biol. **26**, 389 (1961).
[22] S. A. Kauffman, *Lectures on Mathematics in the Life Sciences*, edited by M. Gerstenhaber (American Mathematical Society, Providence, RI, 1971).
[23] L. Glass and S. A. Kauffman, J. Theor. Biol. **39**, 103 (1973).